# Electronic structure and magnetic properties of transition-metal-doped 3*C* and 4*H* silicon carbide

M. S. Miao and Walter R. L. Lambrecht
*Department of Physics, Case Western Reserve University, Cleveland, Ohio 44106-7079, USA*
(Received 19 January 2006; revised manuscript received 12 July 2006; published 28 December 2006)

We report density-functional calculations using the full-potential linearized muffin-tin orbital method on early first row transition-metal-doped silicon carbide in cubic (3*C*) and hexagonal (4*H*) polytypes. The transition energy levels in the gap for Ti, V, and Cr are compared with the available deep level transient spectroscopy and photoluminescence experiments. Our calculation shows that the Ti impurity is active for 4*H* but not for 3*C*, while V and Cr impurities are active for both polytypes. The magnetic interactions are very different for Cr and Mn. Cr shows a very local exchange interaction that decays rapidly after second nearest neighbors, which is similar for different polytypes and different sites. The exchange interaction for Mn is quite long range and is very sensitive to the location of the Mn pairs.

DOI: 10.1103/PhysRevB.74.235218 PACS number(s): 75.50.Pp, 71.55.−i, 71.20.Nr

## I. INTRODUCTION

Silicon carbide is a wide gap semiconductor that has strong potential applications in high-power and high-temperature devices. It is well known for its polytype structure that varies from cubic (3*C*) to wurtzite (2*H*). The most popularly used are the 4*H* and 6*H* polytypes. Early transition metals (TMs), such as titanium, vanadium, and chromium, are common impurities in crystalline SiC grown by the Lely technique and have been thoroughly studied by various experimental methods.[1–8] While impurity related traps are often undesirable, they can also be introduced intentionally to create semi-insulating material. The study of the electronic structures of such defects is important for understanding the nature of the defect levels and so for the design of SiC devices.[9–12,15,16]

The TM impurity levels depend in principle on the polytype and the site (Si or C and possibly cubic or hexagonal site) on which they substitute. For Ti, two levels were observed by deep level transient spectroscopy (DLTS) and found to be very close to the conduction-band minimum (CBM). Actually, DLTS found that the Ti acceptor levels are active for 4*H* SiC but not active for any other polytypes. This places the acceptor level at about 0.15 eV below the 4*H* CBM.[4,17] However, photoluminescence (PL) found this level to be active for 4*H*, 6*H*, and 15*R* but not for 21*R* and 3*C*.[18–20] This places this level at about 0.4 eV below the 4*H* CBM. It is generally accepted that the lower defect level observed by PL is due to the strongly bound exciton effect.

Many experiments have been conducted for V in 4*H* SiC inspired by the fact that V is amphoteric and it can compensate the intrinsic donor and acceptor defects and make semi-insulating SiC samples.[21,22] Both the donor and acceptor levels of V are deep in the gap.[23–26] They are active for all polytypes. The DLTS measurements found the acceptor level at about 0.97 eV below the 4*H* CBM and the donor level at 1.97 eV below the 4*H* CBM state. Cr is also amphoteric and is a possible alternative for V in fabricating semi-insulating SiC. DLTS found two acceptor levels in 4*H* SiC. One is at 0.15 eV and the other at 0.74 eV below the 4*H* CBM.[17,27]

Recently, because of their potential applications in spintronic devices,[28,29] interest has grown in the magnetic properties of TM dopants in various semiconductors and their ability to behave as a dilute magnetic semiconductor (DMS).[30] The main focus has been on III-V host semiconductors[31–34] because divalent TMs such as Mn and Cr substituting on group-III sites act as acceptors and can thus induce hole mediated ferromagnetism. Currently the application is limited by the below room-temperature Curie temperature of most III-V DMSs. A mean-field theory by Dietl and co-workers[35,36] predicted that the semiconductors with light atoms might create stronger magnetic coupling and might be good candidates for room-temperature DMSs. A great amount of experiments have been done for GaN, ZnO, etc. One can also expect the TM doped group-IV semiconductors to be good DMSs because TMs are also acceptors in these hosts. Many studies have been done for III-V and group-IV DMSs,[37–44] however, very few are for SiC,[11–15,45] and none of these works considered the effect of the polytype. In the second part of this work, we study the magnetic properties of Cr and Mn doped 3*C* and 4*H* SiC and discuss how the defect levels and the nature of the defect states will affect the magnetic properties.

## II. METHODOLOGY

The calculations are based on the Kohn-Sham density-functional theory in the local-density approximation (LDA).[46,47] The von Barth-Hedin parametrization[48] is used for the exchange and correlation energy and potential. Supercells with 64 atoms and 72 atoms are used for simulating TM in 3*C* and 4*H* SiC polytypes. The corresponding distances between the image impurities are 8.72 and 9.25 Å, respectively. We used a $4\times4\times4$ *k*-mesh for the structural relaxation of 3*C* cells. For 4*H* cells, we use $2\times2\times2$ *k*-mesh for the relaxation but the final total energies for the optimized structures were performed using a $4\times4\times4$ *k*-mesh. For charged defect states, a uniform neutralizing background is added and a correction is applied for the spurious Madelung energy of an array of point charges in interaction with the background[49] according to the simple procedure suggested by Blöchl.[50] We caution that this correction may be slightly overestimated which would tend to make donor levels too

 ©2006 The American Physical Society

deep below the CBM and the acceptor levels too far above the VBM. Because the defect levels in the gap are primarily localized on the TM $d$ states which are localized, no band-gap shifts are applied to them while we add a gap correction to the conduction-band minimum in displaying the transition energy diagrams.

The calculations are performed using a full potential linearized muffin-tin orbital method[51] (FP-LMTO) which permits analytic calculation of the forces. This method uses a smart and highly efficient basis set consisting of augmented smoothed Hankel function[52] times spherical harmonics centered on the atomic sites. While a muffin-tin approximation is used for the construction of the basis set, the actual all-electron potential and charge density have no shape approximation. The careful choice of smoothing radii and Hankel function energies allows one to use a minimal basis set with at most two functions per angular momentum. As a calibration of the accuracy of the method, we mention that the energy differences between SiC polytypes are reproduced with an accuracy of one-tenth of a meV with a single basis function for $s$, $p$, and $d$ angular momenta compared to more extensive basis sets.[53] For transition metals, we added a second basis function for $s$, $p$, and $d$ angular momentum channels.[54]

## III. RESULTS

### A. Defect levels

The formation energy of TM defects in various charged states are calculated as follows:

$$\Delta H_f(\mathrm{TM}_\alpha^q) = E(\mathrm{SiC{:}TM}_\alpha^q) - E(\mathrm{SiC}) + \mu_{\mathrm{Si}} - \mu_{\mathrm{TM}} + qE_{\mathrm{VBM}} + qE_{\mathrm{F}}. \quad (1)$$

The chemical potentials here are relative to the atomic values, meaning that the energies of the free atoms have already been subtracted from the supercell total energies. The chemical potential of Si varies from the chemical potential of bulk Si, $\mu_{\mathrm{Si}}^b$, equal to the cohesive energy of bulk Si per atom, under Si-rich condition to $\mu_{\mathrm{Si}}^b+\Delta H_f(\mathrm{SiC})$ under C-rich condition, with $\Delta H_f(\mathrm{SiC})=-0.65$ eV (Ref. 15) the energy for formation of SiC from its elements in their bulk state. For the TM, we use the bulk cohesive energy in the elemental metal as chemical potential, which means we consider the system to be in equilibrium with the bulk TM. This is an upper limit for this chemical potential. The last two terms are the contribution from the electron chemical potential $\mu_e=E_{\mathrm{VBM}}+E_F$. $E_{\mathrm{VBM}}$ is the energy of the valence-band maximum (VBM). The latter is given relative to the average electrostatic potential and is determined by aligning the local potential on an atom far away from the defect in the supercell with that of a corresponding bulk atom in the pure material. $E_{\mathrm{F}}$ is the Fermi energy relative the VBM. According to the doping, the Fermi level can change from 0 at the VBM to $E_g$ at the CBM, in which $E_g$ is the band gap. The crossing of the formation energy lines as function of $E_F$ for different charge states gives the defect transition state energy levels. We note that the transition energies do not depend on the chemical potential of Si or the TM. The values for the formation energies presented below correspond all to the Si-poor condition, and TM-rich situation which is the most optimal choice for TM substitution.

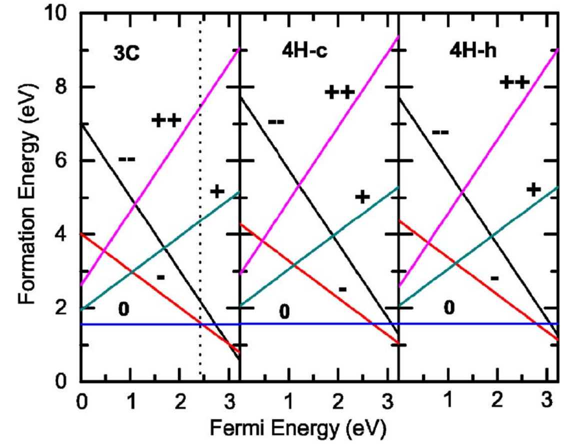


FIG. 1. (Color online) Formation energy of Ti substitution at Si site in 3$C$ and 4$H$ SiC. Five different charged states, including +2, +1, 0, −1, −2, are shown. The two right panels are for Ti in cubic and hexagonal layers in 4$H$ SiC. The energy window extends to 3.23, which equals the band gap of 4$H$ SiC. The vertical dashed line in the left panel indicates the 3$C$ SiC band gap. The (0/+) and the (+/++) transitions for 3$C$ SiC cannot happen because the cross of the lines is higher than the CBM of 3$C$. However, we keep them in the figure to make a comparison with those for 4$H$ SiC.

Figure 1 shows the formation energies for Ti in 3$C$ and in 4$H$ SiC. The formation energy for neutral Ti is about 1.5 eV and there is no significant difference between 3$C$ and 4$H$ nor between the cubic and hexagonal layers in 4$H$ SiC. This indicates that from the energetic point of view, Ti will go equally to both layers in 4$H$. The the transition energies are similar for 3$C$ and 4$H$ SiC. The 0/− level occurs at 2.47 eV for 3$C$ and 2.70 eV for 4$H$. The −/2− level is 3.01 eV for 3$C$ and 3.47 and 3.35 eV for cubic and hexagonal layers in 4$H$. The small differences between 3$C$ and 4$H$ are probably mostly due to systematic differences between the 3$C$ and 4$H$ calculations: since the supercell shapes and sizes are different for 3$C$ and 4$H$ calculations, the corresponding Blöchl corrections are slightly different.[50] We thus refrain from attaching physical significance to these differences. Although the 0/− states are close for 3$C$ and 4$H$ SiC, the band gap of 3$C$ is about 1 eV smaller than 4$H$. The 0/− state lies slightly above the CBM of 3$C$ but 0.3 eV below the CBM of 4$H$ thus making Ti electrically inactive in 3$C$ but active in 4$H$. Note that we can still calculate the negative charge state even if it lies slightly above the conduction-band minimum because of our finite $k$-point sampling with a mesh displaced from Γ, which avoids the actual conduction-band minima, which in the supercell are folded onto Γ. Similar remarks apply to the positive charge states. The +/0 and ++/0 transition states are found to be below the valence-band maximum, which means that they do not actually exist as transition states in the gap.

Figure 2 shows the position of the defect transition energies for Ti, V, and Cr in 4$H$ cubic and hexagonal layers. The levels for TMs in 3$C$ are not shown. They are close to those in 4$H$ except the band gap is now placed at 2.42 eV instead of 3.23 eV.

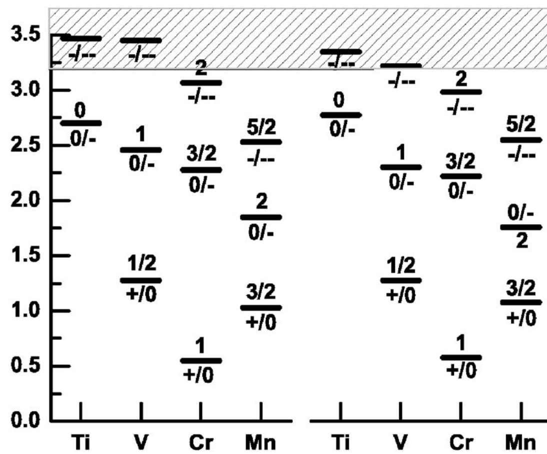


FIG. 2. Early TM defect transition energies at substitutional Si site in $4H$ SiC. Left panel shows such levels in the cubic layers and right panel shows those in the hexagonal layers. Above each level is indicated the spin state that occurs above this level.

Figure 2 shows that Ti has one level in the gap, V has two levels, whereas Cr and Mn have each three levels in the gap. Except for Ti, the other three TMs can act both as donor and acceptor depending on the position of the Fermi level. To understand the defect transition levels, it is useful to examine the single-particle energy levels obtained from the solution of the Kohn-Sham Schrödinger equation, which is most easily done by plotting the partial densities of states (PDOS). For the purpose of displaying these levels, we chose to calculate them for the neutral charge state and the corresponding geometry. Thus the one-electron levels shown do not include the effect of the Coulomb repulsion nor the associated change in geometry relaxation resulting from putting more than one electron in the same degeneratre one-electron level. Nevertheless, the PDOS is useful to identify the major features of the one-electron spectrum and to clarify the origin of the levels in the gap.

Figure 3 shows the PDOS of TMs in $3C$ SiC. The reason why we use the PDOS for $3C$ SiC here is that it allows a straightforward identification of $e$-like spherical harmonics ($d_{x^2-y^2}$, $d_{3z^2-r^2}$) and $t_2$-like ($d_{xy}$, $d_{xz}$, $d_{yz}$) spherical harmonics with $x$, $y$, and $z$ along the cubic axes. For $4H$, the $T_d$ symmetry is broken and one would have to rotate the spherical harmonics locally in each tetrahedron to correspond to those in the cubic case. The states, nevertheless, would still approximately have $e$ and $t_2$ character and the discussion of local bonding would stay the same. In fact, the plots of $l$-resolved PDOS for $4H$ and $3C$ are very similar. The $d$ states of the TM splits into $e$ and $t_2$ symmetry states in a tetrahedral environment. The $t_2$ states can couple with the surrounding dangling bonds because the latter also form $t_2$ symmetry combinations. Since TM $d$ states are higher in energy than the surrounding C dangling bond states, the bonding states of $t_2$ are mainly C $p$ states while the antibonding states are mainly TM $t_2$ $d$ states. Besides the filling of the levels, several trends are important to understand the features of the single-particle levels. First, from Ti to Mn, the average $d$ state levels go down relative to the C states. Second, due to the stronger $d$ to dangling-bond coupling, the splitting becomes larger from Ti to Mn. Last, the spin splitting becomes larger with the number of $d$ electrons. When Ti substitutes for Si in SiC, the bonding $t_2$ states are completely filled, leaving the $e$ states in the gap. The VBM states are mainly C states. Therefore the position of the corresponding acceptor level is determined by the relative position of the Ti $d$ states and C states. Ti has a very high acceptor level because Ti is at the start of the TM series.

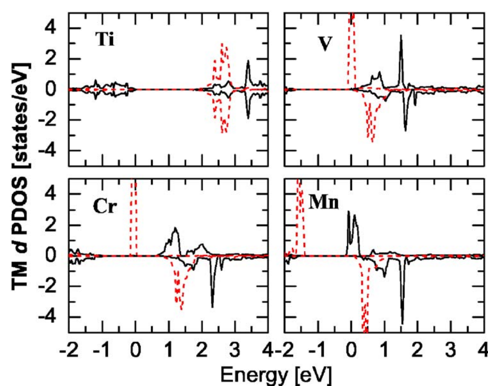


FIG. 3. (Color online) PDOS of neutral charged state of TM at Si site in $3C$ SiC. The Fermi level is set at 0. Black solid line: $t_2$; red dashed line: $e$ symmetry.

Table I shows the actual position of the transition levels in the gap. For Ti substitution, there is only one state in the gap and it is very close to the CBM. However, the position of the state is slightly different for a cubic layer and a hexagonal layer. The DLTS found the split levels to be at 0.16 and 0.12 eV below the CBM. However, our calculations show these levels at 0.53 and 0.46 eV below the CBM. Although we get the correct sequence for the levels of cubic and hexagonal substitutions, our values are about 0.35 eV lower than the DLTS values. Actually these values are closer to the PL results. The three possible sources of errors in the calculation are (i) the geometry relaxation, (ii) the Makov-Payne correction, and (iii) the upward shift of the CBM for correcting the LDA band gap. The geometry relaxation should be reliable for LDA calculations. The neutral state has fully filled bonding $t_2$ levels and empty $e$ levels. Therefore one does not expect any Jahn-Teller symmetry breaking. The negative charged state has one $e$ level occupied and the other empty. Therefore a symmetry breaking will lower the electron energy. However, the calculations show that the effect is small. Furthermore, this effect should tend to lower the energy of negative charged state and thus push the acceptor level even deeper in the gap.

It is commonly known that the Makov-Payne (MP) correction overestimates the image charge effect since the defect charges are not point charges. Therefore the MP correction will push the charged state energy higher. However, this error is considered small for singly charged states. In any case, a more complete correction for the image charge artefacts should lower the energy of the charged state and therefore lower the energy of the acceptor level. Thus it also goes in the wrong direction and would increase the discrepancy between the calculation and the DLTS results.

The last source of error comes from the gap correction. Following usual practice for deep levels, the LDA gap un-

TABLE I. The transition energies (in eV) for Ti, V, Cr, and Mn substitute at cubic ($k$) and hexagonal ($h$) layers in 4$H$ SiC. The values are measured from the conduction-band minimum. The experimental works are DLTS results (Refs. 2, 4, 8, 9, and 27).

| | | Level 1 | | Level 2 | | Level 3 | |
|---|---|---|---|---|---|---|---|
| | | This work | Expt. | This work | Expt. | This work | Expt. |
| Ti | $k$ | 0.53(0/−) | 0.16 | | | | |
| | $h$ | 0.46(0/−) | 0.12 | | | | |
| V | $k$ | 0.90(0/−) | 0.97 | 1.95(+/0) | 1.97 | | |
| | $h$ | 0.93(0/−) | | 1.95(+/0) | | | |
| Cr | $k$ | 0.16(−/2−) | 0.15 | 0.95(0/−) | 0.74(0.53[9]) | 2.68(+/0) | |
| | $h$ | 0.25(−/2−) | 0.18 | 1.01(0/−) | −(0.63[9]) | 2.65(+/0) | |
| Mn | $k$ | 0.70(−/2−) | | 1.38(0/−) | | 2.20(+/0) | |
| | $h$ | 0.68(−/2−) | | 1.47(0/−) | | 2.15(+/0) | |

derestimate is here simply taken into account by shifting the conduction band up to its experimental value without changing the transition energies. However, a state close to the CBM may be expected to have a significant CBM character to its wave function. In other words, if one would project the defect wave function onto the perfect crystal states, there would be a significant overlap or mixing with the CBM. Consequently, if a shift is applied to the CBM, such shallow defect states should also be shifted at least partially along with the CBM. However, it is hard to determine how much these states should shift with the CBM. This problem can only be resolved by treating the gap correction and the defect state at the same footing. The ultimate solution might be to use quasiparticle calculations using the $GW$ approach.[55–57] Unfortunately, this is not yet feasible with current computer power.

As a first step toward this direction, however, we can simulate the effect of GW quasiparticle corrections with shifts of the atomic orbitals primarily involved in the conduction band. In 3$C$ SiC, the conduction-band minimum is at $X$ and experience has shown that these states have a strong Si$s$ and interstital region component. For instance, in the atomic sphere approximation (ASA),[58] they have a strong empty sphere $s$ component.[59] By shifting the Si $s$ and empty sphere $s$ states up in an ASA calculation we can adjust the minimum band gap of SiC to its experimental value. Now, applying the same shifts in the case of the Ti impurity shows that the Ti transition energy shifts up by about 0.6 eV while the conduction-band minimum itself shifts up by about 1 eV. This would place the Ti transition energy just above the conduction-band minimum. However, as noted earlier reducing the overestimate of the Makov-Payne point-charge correction would slightly shift them back down. Although the uncertainties in this approach are too large to determine the level with the desired accuracy, it gives support to the DLTS rather than the PL determined level positions.

For V, the $e$ states are half filled in the neutral charge state and are empty for the positively charged state. The corresponding transition energy is also determined by the relative position of C states and V $d$ states. However, the level is now a donor level. The coupling is also stronger than for Ti. The acceptor level 0/− for V has two electrons filling its $e$ state and its position in the gap relative to the +/0 level is determined by the Coulomb repulsion between the two electrons. The other level that is inside the conduction band is a mixed $e$ and $t_2$ state. It is also worthwhile to notice that the spin splitting for $e$ states is about 0.5 eV.

A sketch of transition levels for V substitution is shown in Fig. 4. The upper and lower shaded areas stand for the valence and the conduction bands of the semiconductor. The VBM and CBM are not lined up in the sketch, which presents the fact that 4$H$ SiC is an indirect semiconductor. The levels at the left side are the transition-metal levels, which are split into $e$ and $t_2$ states. The levels at the right side are the dangling bonds of the carbon atoms at the tetrahedron sites. The four dangling-bond states form one $a_1$ symmetric state which is deep in the valence band and three $t_2$ symmetry states, which are shown in the figure. Due to the symmetry, only $t_2$ $d$ states of the TM will couple with the surround-

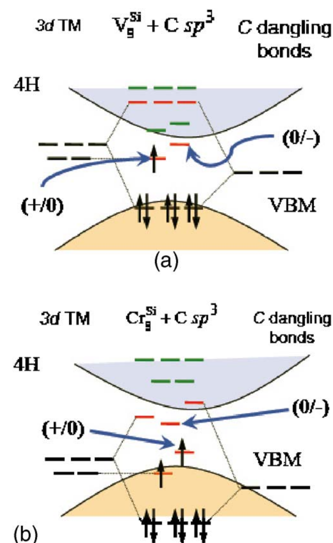


FIG. 4. (Color online) Sketch of the transition levels in the gap for V (top) and Cr (bottom) doped SiC. The energy levels shown include the effects of spin polarization and Coulomb interaction therefore indicate the transition energies.

ing dangling bonds and form bonding and antibonding states. The bonding states have predominantly C dangling-bond contributons and are located deep in the valence bands for V in SiC, while the antibonding states have primarily V *d* character. The *e* states are degenerate and only one is occupied for V in SiC. The spin splitting is shown in the figure and the majority spin levels are lower in energy than the minority spin levels. It is smaller than the $e-t_2$ splitting as indicated by the DOS in Fig. 3. Another splitting between the degenerate *e* states shows the origin of the difference on the transition energies for $(+/0)$ and $(0/-)$ levels. This splitting is caused by the on-site Coulomb interaction.

The calculated V transition energies are also shown in Table I. As shown in the previous paragraph, V is amphoteric and has both acceptor and donor levels in the gap. Our calculation show the acceptor level is 0.90 and 0.93 eV below the CBM for cubic and hexagonal layer substitutions, respectively. The DLTS only resolves one level and is at 0.97 eV below the CBM. The donor level is found by our calculations at 1.95 eV below the CBM for both cubic and hexagonal layer substitutions. Both donor and acceptor levels are in very good agreement with the DLTS results. The success of the density-functional calculations for V in spite of the deficiencies mentioned for the Ti case, is due to the following reasons. First the V levels are all deep in the gap. Second as shown in Fig. 4, top panel, both donor and acceptor levels are *e* states. Such states do not couple well with the surrounding dangling-bond states due to the symmetry mismatch. Thus these states are very localized. Therefore the gap correction by way of shifting the CBM should not affect the positions of these deep levels. Another effect of the strong localization of the defect states is that it is independent of the layer (cubic or hexagonal) in which it sits. As shown by Table I, the position of the acceptor levels has only a 0.03-eV difference in different layers and has no difference for the donor level.

For Cr, the *e* states of the majority spin are completely filled in the neutral state. Its donor level is closer to the VBM as the *d* levels of Cr are lower than V. It has two acceptor levels. The relative position of the $0/-$ level to $+/0$ level is mainly determined by the $e-t_2$ splitting. The spin splitting for *e* states is about 1.2 eV, which is larger than the $e-t_2$ splitting. Therefore both the $-1$ and the $-2$ charged states are in high-spin configuration. (see Fig. 4, bottom panel)

The positions of the first level calculated are at 0.16 and 0.25 eV below the CBM and they are in good agreement with the DLTS results that are at 0.15 and 0.18 eV. Both DFT and DLTS show a slightly lower transition energy for the cubic layer substitution. However, the theoretical value is larger. The energy difference between cubic and hexagonal layer substitutions is more reliable because the systematic errors should be similar for the two cases. The second level measured from the CBM is also an acceptor level and is found at 0.95 and 1.01 eV for cubic and hexagonal layer substitutions, respectively. These values are in poor agreement with the experimental result. This is probably because the Cr acceptor levels are all antibonding $t_2$-like in nature and thus again more sensitive to their environment as discussed above for Ti. They have a strong conduction-band character. Although deep in the gap, they should be affected by the gap correction. This will not explain why the double acceptor level which is much closer to CBM is in better comparison. One possibility is that the overestimation of the MP correction is severe for double negative charge state. It cancels out the error made by the gap correction. Under such consideration, the donor level which is found by calculations at 2.68 and 2.65 eV below the CBM should be more reliable because the donor state is an *e* state and should be localized.

The Mn donor level is an antibonding $t_2$ state. Its majority *e* states lie slightly above the VBM in the PDOS, while its minority *e* state is more than 2 eV above the VBM. Its acceptor states are all antibonding states. The first two levels below the CBM are acceptor levels and the third level is a donor level. We found that the first acceptor level is close to that of V and the acceptor level is also close to the V donor level. Therefore it might be possible to use Mn as an alternative for V to make semi-insulating SiC. However, since all these three defect states are antibonding $t_2$ in character, one should be aware that the DFT supercell calculations might be less reliable due to the strong coupling of the defect states and surrounding dangling-bond states. The large spin splitting of Cr and Mn makes them candidates for dilute magnetic semiconductor (DMS) materials, which will be discussed thoroughly in the next section.

Finally, we compare our results on the energy levels with previous calculations. A few first-principle calculations have been performed for TM in 3*C* and 2*H* SiC, including the recent linearized augmented plane-wave (LAPW) studies.[16,60] The Ti $(0/-)$ transition energy calculated by LAPW is 2.7 eV above the VBM, which is in good agreement with this work. For V, the $(+/0)$ energy is also in good agreement. However, the $(0/-)$ energy is about 0.5 eV lower than our value and the experimental results. The LAPW calculations then obtained a very narrow gap between the two transition energies. A similar trend can be seen for Cr. The $(0/-)$ and the $(+/0)$ energies are in good agreements for both calculations. But the LAPW $(-/2-)$ energy is about 0.5 eV lower than the current result. For Mn, the $(0/-)$ energy is lower and the $(+/0)$ energy is higher than our values. Again the LAPW obtained a significantly smaller energy difference between the $(0/-)$ and the $(+/0)$ levels. This systematic discrepancy might be caused by the neglect of Makov-Payne corrections in the LAPW study. The MP correction will typically increase the energies of the charged states, both negative and positive. Therefore it will enlarge the gap between $(0/-)$ and $(+/0)$.

The V dopant is amphoteric, i.e., it has both donor and accetor levels in the gap. For this reason, V is doped on purpose to make semi-insulating 4*H* SiC because V donor and acceptor levels can passivate both *n*- and *p*-type impurities and greatly lower the carrier concentration. It is obvious that a good amphoteric dopant for the above purpose should have a higher donor level so it can passivate all the acceptor levels below it. On the other hand, its acceptor level should be low enough so that it can passivate all the donor levels above it. Therefore a good candidate dopant for making semi-insulating SiC should have close donor and acceptor levels. V fulfills this role because the energy difference between its acceptor and donor levels is determined by the on-site Coulomb interaction between two electrons occupy-

ing the degenerate $e$ states. The corresponding splitting is significantly smaller than the $e-t_2$ splitting. Cr is also amphoteric, as shown by Fig. 2. However, the energy difference that seperates the donor and acceptor levels results from the $e-t_2$ splitting. This is the reason that the energy difference between the donor and the acceptor states are significantly larger for Cr. On the other hand, the Cr donor level is very low in the gap because the position of this level is determined by the splitting of the two $e$ states, which in turn is caused by the on-site Coulomb interaction. For all these reasons, Cr is not a good candidate for making semi-insulating 4*H* SiC. From our calculation, we found that Mn is also a good candidate for making a semi-insulating 4*H* SiC. It is amphoteric and its donor level is high whereas its acceptor level is low. The energy difference between its acceptor and donor levels are determined by Coulomb interaction between the electrons occupying the degenerate $t_2$ states and therefore is as small as that of V. As shown in Fig. 2, Mn has two acceptor levels. It might be a more effective candidate than V for making semi-insulating 4*H* SiC, especially for passivating the *n*-type impurities.

One important issue that we did not discuss so far is the geometry relaxation and the possible Jahn-Teller distortion. The relaxation and the possibility of a Jahn-Teller distortion are fully included in our calculation, i.e., we always start from an initial geometry that breaks the symmetry. In several neutral or charged defect states, the degenerate $e$ or $t_2$ states are partially filled and therefore one expects that a Jahn-Teller distorsion could lower the energy by splitting the degenerate states. However, in 4*H*, we already have a symmetry lowering from $T_d$ to $C_{3v}$ as the local point group even without distortion, so the degeneracy argument no longer applies. For example, Mn defect has three electrons in the gap states. For cubic system, two of them occupy the $e$ states and the other one occupies one of the triply degenerate $t_2$ states. However, under $C_{3v}$ symmetry, the degenerate $t_2$ states break into one $a_1$ state and two $e$ states. The $a_1$ state is lower in energy than the $e$ states. Our calculations show that the system does not show a Jahn-Teller distortion within the accuracy of the calculation and remains in $C_{3v}$ symmetry. This is also true for all the other defect states. Due to small numerical errors, we typically find very slight deviations from perfect symmetry but these are within the error margin of the calculations. The largest distortions observed are for the $-2$ charged state of V and Cr, and are both about 0.3%. Furthermore, because the size of the transition-metal ions fits very well the size of the Si site, even the breathing distortion (maintaining the symmetry) is usually small. The changes of the TM-C bond length before and after relaxation is usually less than 3%. This is quite small in comparison with the relaxation of vacancies in SiC, which is usually around 10%.

### B. Magnetic properties of Cr and Mn in SiC

Transition-metal dopants in semiconductors can potentially lead to dilute magnetic semiconductors if certain conditions are satisfied: (i) we need magnetic moments on the individual TM impurities, (ii) the exchange coupling between them should prefer parallel alignment of spins, (iii) the exchange interactions must be of sufficiently long range, and (iv) a sufficiently large concentration of TM dopants can be incorporated without creating secondary phases. The last two of these are clearly inter-related. In order to establish long-range magnetic order, the concentration must be above the percolation threshhold for a given range of interactions.

The nature of ferromagnetic exchange in the currently much studied III-V dilute magnetic semiconductors is still much under discussion. One school of thought[35] is that the divalent TM dopants introduce both a local spin and a delocalized hole. There is then a hole-mediated exchange coupling between the local spins, usually described in terms of a Ruderman-Kittel-Kasuya-Yosida (RKKY) model. This model to some extent applies to GaAs:Mn because in that case, the TM transition levels are close to the valence-band maximum. On the other hand, if the TM transition levels lie deep in the gap as is the case in GaN:Mn, then a more local exchange coupling mechanism must be invoked and the transport does not occur via delocalized carriers but by activated hopping in an impurity band. The distinction between these two cases was recently discussed by Mahadevan and Zunger.[43] The consequences of these models for critical temperatures are still far from clear. The hole mediated mechanism has suggested some clear guidelines: for instance, reducing the compensation by *n*-type interstitial Mn by annealing treatments has achieved significant improvements in the critical temperature. Nevertheless, a maximum $T_c$ of about 150 K seems to have been reached for Mn-doped GaAs. On the other hand, this same model has predicted higher $T_c$ by going towards lower atomic number semiconductors with smaller lattice constants and hence stronger exchange couplings.[35,61] This, however, is subject to criticism because the model itself may no longer be applicable.[43,62–64] The experimental side is also rather unclear at present because of the uncertainties related to possible secondary phases being at least in part responsible for the magnetic behavior. As a starting point for considering the situation in SiC, we here discuss each of the above requirements in succession. As we will see shortly, Mn and Cr in SiC are more resemblant to the case of GaN than GaAs but also shows some unique differences because we deal with a IV-IV compound as host.

First, it is already clear from the previous section that magnetic moments do occur on the individual TM ions. In fact, we note that in contrast to our earlier study of TM dopants in 3*C* SiC,[15] which used mainly the atomic sphere approximation and did not include lattice relaxation effects around the impurities, we find here high-spin states for all the TM impurities under study. In our earlier study, we had found that some cases corresponded to a low-spin configuration because the magnetism was found to be in competition with covalent bonding and hence the crystal-field splitting could exceed the exchange splitting. Our present more accurate calculations, however, did not confirm this. Presumably, this is mostly due to the inclusion of lattice relaxation but other technical aspects of the calculation, such as *k*-point convergence, full-potential vs ASA also may play a role.

As shown in the previous section, the early TM dopants in SiC: V, Cr, and Mn can behave both as donor and as acceptor. Their acceptor levels are either deep in the gap or close

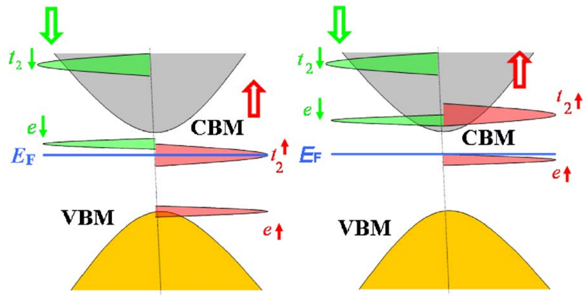


FIG. 5. (Color online) Sketch of the defect bands in SiC gap for Mn (left) and Cr (right) doped 4$H$ SiC.

to the CBM. Therefore the doping of TM in SiC cannot induce delocalized holes, excluding the hole mediated exchange coupling mechanism. However, the local spins may still couple through local exchange interactions. As already pointed out by Mahadevan and Zunger[43] the orbital character or symmetry of the impurity levels in the gap containing the unpaired electrons is an important consideration in determining whether the exchange interactions will be short-ranged or long-ranged. Figure 5 shows a sketch of the impurity bands in the gap of SiC. Although the defect levels for Cr and Mn are all deep in the gap, their nature is different. For SiC:Cr, the majority spin $e$ states are fully occupied whereas the antibonding $t_2$ states are empty. For SiC:Mn, there is one more electron and it starts to occupy the antibonding $t_2$ state of the majority spin channel. Therefore the unpaired spin resides in states of different symmetry for Mn and for Cr. It is worthwhile to notice that in III-V semiconductors, the electrons start to occupy the antibonding $t_2$ states for the Cr-doped system since there is one more electron in comparison with the group-IV semiconductor DMS. It is interesting to check the magnetic behavior of Cr-doped SiC since its $e$ state derived magnetic moment is unique for group-IV semiconductors. An $e$ state would occur for V in III-$N$ but the latter has smaller exchange splitting and is not found to lead to ferromagnetism.

To study the magnetic coupling, we calculated the total energy of supercells of 3$C$ and 4$H$ SiC which contain two Cr or Mn substitutions at Si sites in various configurations. We are primarily interested in the energy difference between the ferromagnetic (FM) and the antiferromagnetic (AFM) states as it reveals the strength of the magnetic coupling between neighboring dopants. We show the energy difference in Fig. 6. For SiC:Cr, the energy differences are very large for the first neighbors and quickly decrease to almost zero for second and third nearest neighbors. Another important feature is that the energy difference does not depend on the polytype and also not on the choice of cubic or hexagonal site within the 4$H$ polytype. The SiC:Mn system shows a totally different behavior. The absolute values of the energy difference between FM and AFM states are smaller, on the other hand they are longer range in comparison with SiC:Cr. It also shows a different pattern in the 3$C$ and 4$H$ polytype. Recently, the Cr- and Mn-doped 3$C$ SiC have also been studied by the ultrasoft pseudopotential method.[13,14] The energy difference between FM and AFM states are much larger than ours (see Table I of Ref. 14).

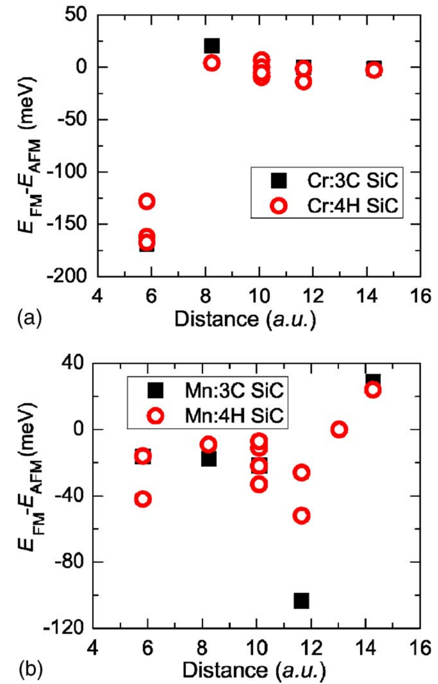


FIG. 6. (Color online) Total energy difference between FM and AFM states for Cr and Mn in SiC at different neighbors.

Within the 64 atoms cell for 3$C$ and 72 atoms cell for 4$H$, one can extract the magnetic coupling parameters up to sixth nearest neighbors by mapping the energy differences to a Heisenberg exchange model. Interestingly, the neighboring distances are very similar for 3$C$ and 4$H$ polytypes. They are listed in Table II. If the dopant sits in a hexagonal layer in 4$H$, then the distances to its neighbor sites are identical to those for a dopant in 3$C$ SiC. If the dopant is in a cubic layer of 4$H$ SiC, then the third, fourth, and sixth neighbors split into two groups with slightly different distances. One might at first expect that the dopant in a cubic layer of 4$H$ should have identical neighbors as the dopants in 3$C$. However, the neighbor distances are determined by the neighboring layers. When the dopant is on the hexagonal layer of 4$H$, its two neighboring layers are all cubic. When the dopant is on a cubic layer, its two neighboring layers are both hexagonal. Therefore the neighbor distances are identical to 3$C$ while the dopant is in a hexagonal layer. Since the splitting of the distances is very small while the dopant is in the cubic layer

TABLE II. The distances between neighboring dopants (in units of the cubic lattice constant) and the corresponding $J$ parameters. The notation NN1 stands for first nearest neighbor, etc.

| Neighbors | Exchange | 3$C$ | 4$H$-$h$ | 4$H$-$k$ |
|---|---|---|---|---|
| NN1 | $J_1$ | 1 | 1 | 1 |
| NN2 | $J_2$ | $\sqrt{2}$ | $\sqrt{2}$ | $\sqrt{2}$ |
| NN3 | $J_3$ | $\sqrt{3}$ | $\sqrt{3}$ | $\sqrt{3}$, $\sqrt{8/3}$ |
| NN4 | $J_4$ | 2 | 2 | 2, $\sqrt{11/3}$ |
| NN5 | $J_5$ | $\sqrt{5}$ | $\sqrt{5}$ | $\sqrt{5}$ |
| NN6 | $J_6$ | $\sqrt{6}$ | $\sqrt{6}$ | $\sqrt{6}$, $\sqrt{17/3}$ |

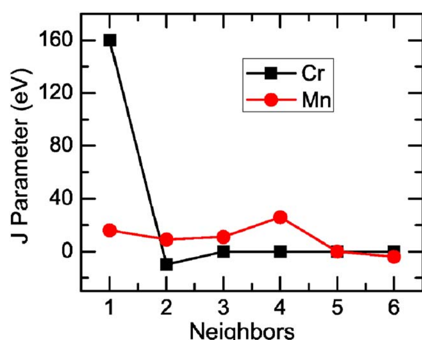


FIG. 7. (Color online) Exchange coupling constants for Cr and Mn in 4$H$ SiC at different neighbors.

of 4$H$, we neglect it and treat them with the same coupling parameters, $J_3$, $J_4$, and $J_6$. Furthermore, the exchange interactions can in principle depend on orientation and random effects due to the presence of other magnetic atoms farther away,[63] rather than simply on distance. These aspects will need further study.

Figure 7 presents the extracted magnetic coupling parameters for Cr and Mn in both 3$C$ and 4$H$ SiC. Although both ferromagnetic, the magnetic couplings are very different for Cr and Mn. Cr shows a very short-range coupling that decays quickly to zero beyond the first nearest neighbor. On the other hand, Mn shows longer range interactions that are ferromagnetic up to fourth nearest neighbor. This difference can be understood by the nature of the defect state. The range of the magnetic interaction is determined by the nature of the defect state. As explained in the previous section, the electrons in the neutral Cr dopants are in $e$ state, whereas for Mn they are in antibonding states. The later states couple stronger with the surrounding atoms and therefore are more delocalized. To show the localization of these states, we calculated the charge density of the neutral Cr and Mn dopants integrated within the energy windows that embrace the $e$ states for Cr and the occupied antibonding states for Mn. The isosurface of the charge densities are shown in Fig. 8. They are picked at equal density for Cr and Mn (corresponding to 2% and 1% of the peak density in the grid). Figure 8 clearly shows that the Cr state is very local and the Mn state spreads out to at least fourth neighbors. Another important feature is the direction of the wave function lobes. For Cr, it points to $x$, $y$, and $z$ directions whereas for Mn it points toward the diagonal directions. This is because the electrons occupy the $e$ states in Cr and the $t_2$ states in Mn. Therefore the Mn occupied state can couple effectively with the surrounding C states and induce stronger magnetic interactions with longer range.

Although our calculations show the couplings for Cr and Mn in SiC are mainly ferromagnetic, this is not sufficient to consider Cr- and Mn-doped SiC as good DMS candidates. Cr has strong but very short-range magnetic coupling. Therefore in the dilute doping limit it is hard to reach the percolation limit required for ferromagnetism. The magnetic interactions for Mn in SiC are longer range but an order of magnitude smaller than those of Cr in SiC and are also considerably smaller than those for Mn doped GaAs, GaN, etc. In addition, one needs to consider the competition of dilute impurities with the formation of carbides and silicides. This aspect was considered in Ref. 15 and although among TM, Mn and Cr and not strong carbide formers, which is favorable for the Si substitution, silicide formation is still an issue in limiting the chemical potentials that are allowed for the TM. Nevertheless, further experimental work on TM doping of SiC would be desirable. The complementary nature of Cr and Mn in terms of their defect wave functions suggest it might be

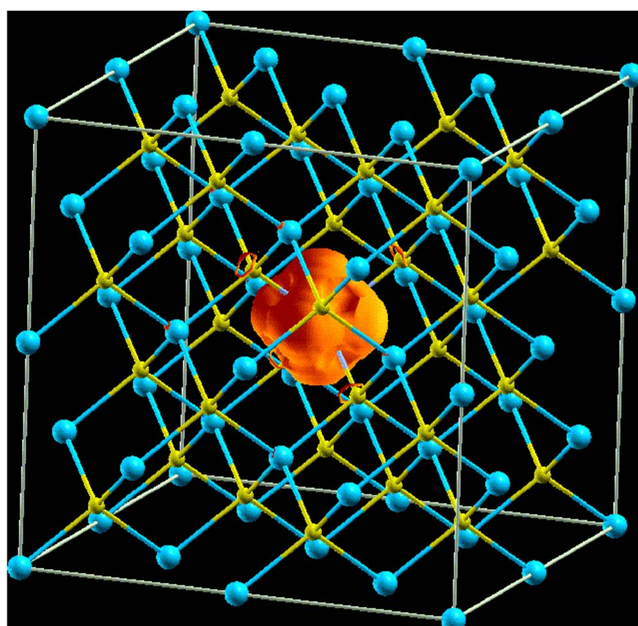

(a)

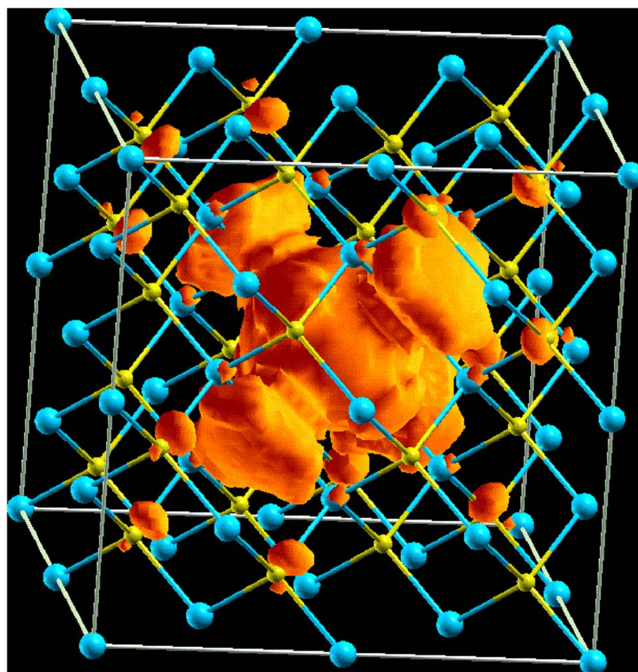

(b)

FIG. 8. (Color online) Charge density isosurfaces of the defect states for (a) Cr and (b) Mn in 3$C$ SiC. The large spheres are Si and the small spheres are C. The Cr and the Mn are at the center of the cell. Figure made with XCrySDen (Ref. 65).

possible to increase the range and the strength of the magnetic interactions by co-doping Cr and Mn.

## IV. CONCLUSIONS

We calculated the impurity transition energies of the early transition metals (Ti, V, Cr, Mn) in $4H$ and $3C$ SiC. We found that the values of the transition energies in the gap are determined by the relative position of the TM $d$ states to C states, the crystal-field splitting, and the spin polarization. The transition energies change only slightly for different polytypes and with the cubic or hexagonal site in $4H$. However, since there is a large difference in energy gap between these polytypes, the activity of the defect states can be different in $3C$ and $4H$. The number of different defect levels, their associated spin spates, and positions in the gap compare favorably with experimental data as long as the levels are deep enough that gap corrections do not play a major role. For Ti, which has transition levels close to the conduction-band minimum, corrections beyond LDA in the defect calculation were found to be important. As far as magnetic properties are concerned, we found that both Mn and Cr occur in high-spin states with magnetic moments of $3\mu_B$ and $2\mu_B$, respectively in the neutral state. We also found that because the highest occupied state for Cr and Mn dopants have different symmetry, the strength and the range of the magnetic coupling differ significantly for the two dopants. While both prefer ferromagnetic coupling, it is strong but short ranged for Cr due to the $e$ character of the impurity state, and smaller but long ranged for Mn.

## ACKNOWLEDGMENTS

This work was supported by the Office of Naval Research under Grant No. N0004-02-1-0880 and the National Science Foundation under Grant No. ECS-0223634.

[1] J. Schneider and K. Maier, Physica B **185**, 199 (1993).
[2] M. Kunzer, H. D. Müller, and U. Kaufmann, Phys. Rev. B **48**, 10846 (1993).
[3] J. M. Spaeth, S. GreulichWeber, M. Marz, J. Reinke, M. Fleege, E. N. Kalbukhova, and S. N. Lukin, Mater. Sci. Forum **239-241**, 149 (1997).
[4] T. Dalibor, G. Pensl, N. Nordell, and A. Schöner, Phys. Rev. B **55**, 13618 (1997).
[5] J. Baur, M. Kunzer, and J. Schneider, Phys. Status Solidi A **162**, 153 (1997).
[6] N. Achtziger, J. Grillenberger, and W. Witthuhn, Mater. Sci. Forum **264-268**, 541 (1998).
[7] A. A. Lebedev, Semiconductors **33**, 107 (1999).
[8] J. Grillenberger, N. Achtziger, G. Pasold *et al.*, Mater. Sci. Forum **389-393**, 573 (2002).
[9] G. Pasold, N. Achtziger, J. Grillenberger *et al.*, Mater. Sci. Forum **353-356**, 471 (2000).
[10] H. Overhof, Mater. Sci. Forum **258-263**, 677 (1997).
[11] V. L. Shaposhnikov and N. A. Sobolev, J. Phys.: Condens. Matter **16**, 1761 (2004).
[12] I. I. Parfenova, Semiconductors **38**, 189 (2004).
[13] Y.-S. Kim and Y.-C. Chung, IEEE Trans. Magn. **41**, 2733 (2005).
[14] Y.-S. Kim, Y.-C. Chung, and S.-C. Yi, Mater. Sci. Eng., B **126**, 194 (2006).
[15] M. S. Miao and W. R. L. Lambrecht, Phys. Rev. B **68**, 125204 (2003).
[16] L. V. C. Assali, W. V. M. Machado, and J. F. Justo, Phys. Rev. B **69**, 155212 (2004).
[17] N. Achtziger and W. Witthuhn, Mater. Sci. Eng., B **46**, 333 (1997).
[18] L. Patrick and W. J. Choyke, Phys. Rev. B **10**, 5091 (1974).
[19] A. W. C. Kemenade and S. H. Hagen, Solid State Commun. **14**, 1331 (1974).
[20] K. M. Lee, L. S. Dang, G. D. Watkins, and W. J. Choyke, Phys. Rev. B **32**, 2273 (1985).
[21] H. McD. Hobgood, R. C. Glass, A. Augustine, R. H. Hopkins, J. Jenny, M. Skowronski, W. C. Mitchel, and M. Roth, Appl. Phys. Lett. **66**, 1364 (1995).
[22] W. C. Mitchel, M. D. Roth, A. O. Evwaraye, P. W. Yu, S. R. Smith, J. Jenny, M. Skowronski, H. McD. Hobgood, R. C. Glass, A. Augustine, and R. H. Hopkins, Inst. Phys. Conf. Ser. **142**, 313 (1996).
[23] K. Maier, H. D. Muller, and J. Schneider, Mater. Sci. Forum **83-87**, 1183 (1992).
[24] K. Maier, J. Schneider, W. Wilkening, S. Leibenzeder, and R. Steine, Mater. Sci. Eng., B **11**, 27 (1992).
[25] K. F. Dombrovskii, U. Kaufman, and M. Hunzer, Appl. Phys. Lett. **65**, 184 (2004).
[26] J. Schneider, H. D. Muller, K. Maier, W. Wilkening, F. Fuchs, A. Dornen, S. Leibenzader, and S. Steine, Appl. Phys. Lett. **56**, 1184 (1990).
[27] N. Achtziger and W. Witthuhn, Phys. Rev. B **57**, 12181 (1998).
[28] G. A. Prinz, Phys. Today **48** (4), 48 (1995).
[29] G. A. Prinz, Science **282** (5394), 1660 (1998).
[30] K. C. Hass, in *Semimagnetic Semiconductors and Diluted Magnetic Semiconductors*, edited by Michel Averous and Minko Balkanski (Plenum, New York, 1991), p. 59.
[31] H. Munekata, H. Ohno, S. von Molnar, Armin Segmuller, L. L. Chang, and L. Esaki, Phys. Rev. Lett. **63**, 1849 (1989).
[32] H. Ohno, A. Shen, F. Matsukura, A. Oiwa, A. Endo, S. Katsumoto, and Y. Iye, Appl. Phys. Lett. **69**, 363 (1996).
[33] Y. Ohno, D. K. Young, B. Beschoten, F. Matsukura, H. Ohno, and D. D. Awschalom, Nature (London) **402**, 790 (1999).
[34] H. Ohno, Science **281**, 951 (1998).
[35] T. Dietl, H. Ohno, F. Matsukura, J. Cibert, and D. Ferrand, Science **287**, 1019 (2000).
[36] T. Dietl, H. Ohno, and F. Matsukura, Phys. Rev. B **63**, 195205 (2001).
[37] H. Akai, Phys. Rev. Lett. **81**, 3002 (1998).
[38] T. Ogawa, T. Shirai, N. Suzuki, and I. Kitagawa, J. Magn. Magn. Mater. **196-197**, 428 (1999).
[39] S. Sanvito, P. Ordejón, and N. A. Hill, Phys. Rev. B **63**, 165206 (2001).
[40] Yu-Jun Zhao, W. T. Geng, K. T. Park, and A. J. Freeman, Phys.

Rev. B **64**, 035207 (2001).

[41] M. Jain, L. Kronik, J. R. Chelikowsky, and V. V. Godlevsky, Phys. Rev. B **64**, 245205 (2001).

[42] M. van Schilfgaarde and O. N. Mryasov, Phys. Rev. B **63**, 233205 (2001).

[43] P. Mahadevan and A. Zunger, Phys. Rev. B **69**, 115211 (2004).

[44] Y. D. Park, A. T. Hanbicki, S. C. Erwin, C. S. Hellberg, J. M. Sullivan, J. E. Mattson, T. F. Ambrose, A. Wilson, G. Spanos, and B. T. Jonker, Science **295**, 651 (2002).

[45] S. J. Pearton, Y. D. Park, C. R. Abernathy *et al.*, Thin Solid Films **447**, 493 (2004).

[46] P. Hohenberg and W. Kohn, Phys. Rev. **136**, B864 (1964).

[47] W. Kohn and L. J. Sham, Phys. Rev. **140**, A1133 (1965).

[48] U. von Barth and L. Hedin, J. Phys. C **5**, 2064 (1972).

[49] G. Makov and M. C. Payne, Phys. Rev. B **51**, 4014 (1995).

[50] P. E. Blöchl, Phys. Rev. B **62**, 6158 (2000).

[51] M. Methfessel, M. van Schilfgaarde, and R. A. Casali, in *Electronic Structure and Physical Properties of Solids, The Uses of the LMTO Method*, edited by H. Dreysse, Springer Lecture Notes, Workshop Mont Saint Odille, France, 1998 (Springer, Berlin, 2000), p. 114.

[52] E. Bott, M. Methfessel, W. Krabs, and P. C. Schmidt, J. Math. Phys. **39**, 3393 (1998).

[53] S. Limpijumnong and W. R. L. Lambrecht, Phys. Rev. B **57**, 12017 (1998).

[54] M. S. Miao and W. R. L. Lambrecht, Phys. Rev. B **71**, 214405 (2005).

[55] L. Hedin and S. Lundqvist, Solid State Phys. **23**, 1 (1969).

[56] F. Aryasetiwan and O. Gunnarsson, Rep. Prog. Phys. **61**, 237 (1998).

[57] S. V. Faleev, M. van Schilfgaarde, and T. Kotani, Phys. Rev. Lett. **93**, 126406 (2004).

[58] O. K. Andersen, Phys. Rev. B **12**, 3060 (1975).

[59] N. E. Christensen, Phys. Rev. B **30**, 5753 (1984).

[60] W. V. M. Machado, J. F. Justo, and L. V. C. Assali, Mater. Sci. Forum **483-485**, 531 (2005).

[61] S. C. Erwin and C. S. Hellberg, Phys. Rev. B **68**, 245206 (2003).

[62] S. Y. Wu, H. X. Liu, L. Gu, R. K. Singh, L. Budd, M. van Schilfgaarde, M. R. McCartney, D. J. Smith, and N. Newman, Appl. Phys. Lett. **82**, 3047 (2003).

[63] J. L. Xu, M. van Schilfgaarde, and G. D. Samolyuk, Phys. Rev. Lett. **94**, 097201 (2005).

[64] M. van Schilfgaarde and O. N. Mryasov, Phys. Rev. B **63**, 233205 (2001).

[65] A. Kokalj, Comput. Mater. Sci. **28**, 155 (2003); code available from http://www.xcrysden.org/